Physical Science International Journal
12(4): 1-11, 2016; Article no.PSIJ.29926
ISSN: 2348-0130

SCIENCEDOMAIN *international*
www.sciencedomain.org

MHD Stagnation Point Flow and Heat Transfer of a Nanofluid over a Non-isothermal Stretching Sheet in Porous Medium

G. Vasumathi[1*], J. Anand Rao[2] and B. Shankar[2]

[1]Research Scholar, Department of Mathematics, Osmania University, Hyderabad, India.
[2]Department of Mathematics, Osmania University, Hyderabad, India.

Authors' contributions

This work was carried out in collaboration between all authors. Author GV designed the study, wrote the protocol, wrote the first draft of the manuscript, managed the literature searches and analyses of the study performed the spectroscopy analysis. Authors JAR and BS managed the experimental process and identified the species of plant. All authors read and approved the final manuscript.

Article Information

DOI: 10.9734/PSIJ/2016/29926
Editor(s):
(1) Alexander Tolstoguzov, Department of Physics, Universidade Nova de Lisboa, Portugal.
(2) Aleksey Anatolievich Zakharenko, The International Institute of Zakharenko Waves (IIZWs), Krasnoyarsk, Siberia, Russia.
(3) Christian Brosseau, Distinguished Professor, Department of Physics, Université de Bretagne Occidentale, France.
Reviewers:
(1) John Abraham, University of St. Thomas, USA.
(2) Munir Ahmed G. Timol, Veer Narmad South Gujarat University, India.
Complete Peer review History: http://www.sciencedomain.org/review-history/16924

Original Research Article

Received 4th October 2016
Accepted 7th November 2016
Published 14th November 2016

ABSTRACT

The present study deals with the MHD stagnation point flow of Nanofluid past a non-isothermal stretching sheet in porous medium. The presence of Brownian motion and thermophoresis effects yields a coupled nonlinear Boundary Value Problem. The sheet is assumed to be permeable. Similarity transformations are invoked to reduce the partial differential equations into higher order nonlinear ODE's. The transformed equations are solved numerically by using a well known finite difference scheme Keller-Box method. The analysis has been carried out for two different cases, namely prescribed surface temperature (PST) and prescribed heat flux (PHF) to see the effects of governing parameters for various physical conditions. The various non dimensional parameters effects with velocity, temperature and concentration profiles are discussed in detail with graphically and tabular form. The results indicate that increasing the Brownian motion parameter and thermophoresis parameter reduces the heat transfer rate at the surface. Increasing porosity parameter reduces the velocity of nanofluid and increases the temperature of nanofluid.

**Corresponding author: E-mail: gandamallavasumathi@gmail.com;*

Keywords: Nanofluid; MHD; non-isothermal stretching sheet; stagnation point; heat transfer; porous medium.

1. INTRODUCTION

Choi [1] was the former who introduced the term of Nanofluid to explain the new class of nanotechnology based heat transfer fluids engineered by typical length scales on the order of 1 to 100 nm in traditional heat transfer fluids. The presence of the nanoparticles in the fluids increases significantly the effective thermal conductivity of the fluid, and consequently enhances the heat transfer characteristics, which is observed by Masuda et al. [2]. Buongiorno. J. [3] explained the effect of seven slip mechanisms: inertia, Brownian diffusion, thermophoresis, diffusiophoresis, Magnus effect, fluid drainage and gravity setting. M. Eldabe et al. [4] studied the Effect of magnetic field on flow and heat transfer over an unsteady stretching surface embedded in a porous medium filled with nanofluid. Similarity solutions to viscous flow and heat transfer of nanofluid over nonlinearly stretching sheet are examined by M. A. Hamad and Ferdows M. [5].

The industrial manufacturing processes like wire and fiber coating and transpiration cooling etc., require the study of MHD flow. Basically the MHD flow has wide applications in Engineering and industrial fields. The study of MHD flow of an electrically conducting fluid due to a stretching sheet is important in modern metallurgy and metal-working process. So this study has gained considerable attention in the recent years.

Magnetohydrodynamics and boundary layer flow over a stretching sheet were numerically studied by Fadzilah et al. [6] and Ishak et al. [7] and their investigation showed that flow field velocity at a point decreases with an increase in the magnetic field due to Lorenz force effect. Likewise, researchers such as Mahapatra and Gupta [8] and Ishak et al. [9] extended the dimension of MHD boundary layer flow over a stretching sheet in different types of fluid such as micro polar fluids and power-law fluids with various flow geometries. Mabood et al. [10] studied the MHD boundary layer flow and heat transfer of nanofluids over a nonlinear stretching sheet. Shankar et al. [9] investigated radiation and mass transfer effects on MHD free convection fluid flow embedded in a porous medium with heat generation/absorption.

The study of MHD stagnation point flow on stretching sheet has attracted many researchers in recent times, and many problems as regards different aspects, including the stretching sheet with variable surface temperature [11] or viscous dissipation [12,13], the effects of slip [14], and the analysis of the unsteady case [15]. Effects of radiation and magnetic field on the mixed convection stagnation-point flow over a vertical stretching sheet in a porous medium considered by Hayat et al. [16]. Recently, Ibrahim and Shankar [17] have analyzed MHD boundary layer flow and heat transfer of a nanofluid past a permeable stretching sheet with velocity, thermal and solutal slip boundary conditions. Roslinda Nazar [18] analyzed Unsteady mixed convection boundary layer flow near the stagnation point on a vertical surface in a porous medium.

During the past several decades the study of flow over a non isothermal stretching sheet as attended many investigations. It has wide applications in many industrial and engineering fields. MHD Flow and Heat Transfer past a Porous Stretching Non-Isothermal Surface in Porous Medium with Variable Free Stream Temperature is studied by Swathi [19]. P.S. Datti et al. [20] have investigated MHD visco-elastic fluid flow over a non-isothermal stretching sheet. K.V. Prasad et al. [21] discussed Momentum and heat transfer in visco-elastic fluid flow in a porous medium over a non-isothermal stretching sheet.

Motivated by these studies, in this paper, we analyzed the problem of MHD stagnation point flow and heat transfer of a nanofluid over a non-isothermal stretching sheet in porous medium by considering the effects of Brownian motion and Thermophoresis parameters numerically by adopting the well known Keller-Box method. In addition this study has important applications in several manufacturing process from industry, a variety of engineering, astrophysical and geophysical problems.

In this investigation, we consider two general cases of non-isothermal boundary conditions:

(i) Prescribed surface temperature (PST)
(ii) Prescribed surface heat flux (PHF)

The effects of governing parameters on fluid velocity, temperature and particle concentration have been discussed. To verify the obtained results, I have compared the present numerical results with previous work by Ibrahim [22] and a very good agreement has been established.

2. MATHEMATICAL FORMULATION

Consider the steady, two-dimensional laminar boundary layer flow of nanofluid in the region of stagnation point towards a non isothermal stretching sheet in a porous medium situated at $y = 0$ as shown in Fig. 1. The X – axis and Y – axis are taken along and perpendicular to the sheet and the flow is confined to $y \geq 0$. The effects of Brownian motion and thermophoresis are also accounted.

The stretching velocity $U_w(x)$ and the free stream velocity $U_\infty(x)$ are assumed to vary proportional to the distance x from the stagnation point, i.e. $U_w(x) = ax$ and $U_\infty = bx$, where a and b are constants with $a > 0$ and $b \geq 0$. It is also assumed that the surface of the sheet is subjected to a prescribed temperature $T_w = T_\infty + Ax^n$, where T_∞ is the ambient fluid temperature and A and n are constants with $A > 0$ (heated surface). Further, a uniform magnetic field of strength is assumed to be applied in the positive y-direction normal to the stretching sheet. The magnetic Reynolds number is assumed to be small, and thus the induced magnetic field is negligible.

The simplified two-dimensional equations governing the flow of a steady, boundary layer flow are considered as:

$$\frac{\partial u}{\partial x} + \frac{\partial v}{\partial y} = 0 \tag{1}$$

$$u\frac{\partial u}{\partial x} + v\frac{\partial u}{\partial y} = U_\infty \frac{dU_\infty}{dx} + \upsilon \frac{\partial^2 u}{\partial y^2} - \frac{\sigma {B_0}^2}{\rho}(u - U_\infty) - \frac{\upsilon}{k1}u \tag{2}$$

$$u\frac{\partial T}{\partial x} + v\frac{\partial T}{\partial y} = \alpha \frac{\partial^2 T}{\partial y^2} - \frac{1}{(\rho c)_f}\frac{\partial q_r}{\partial y} + \tau[D_B \frac{\partial C}{\partial y}\frac{\partial T}{\partial y} + \frac{D_T}{T_\infty}\left(\frac{\partial T}{\partial y}\right)^2] \tag{3}$$

$$u\frac{\partial \phi}{\partial x} + v\frac{\partial \phi}{\partial y} = D_B \frac{\partial^2 \phi}{\partial y^2} + \frac{D_T}{T_\infty}\frac{\partial^2 T}{\partial y^2} \tag{4}$$

The velocity and concentration boundary conditions are:

$$u = U_w(x) = ax,\ v = 0,\ \phi = \phi_w \quad at\ \ y = 0,$$
$$u \longrightarrow U_\infty = bx,\ \ v = 0,\ \ \phi = \phi_\infty \quad as\ \ y \longrightarrow \infty. \tag{5}$$

The thermal boundary conditions are:

(i) The prescribed surface temperature

$$T = T_w = T_\infty + Ax^n, \quad at\ y = 0,$$
$$T \longrightarrow T_\infty\ as\ y \longrightarrow \infty. \tag{6}$$

(ii) The prescribed heat flux

$$-k\frac{\partial T}{\partial y} = q_w = Dx^s \quad at\ y = 0,$$
$$T \longrightarrow T_\infty\ as\ y \longrightarrow \infty. \tag{7}$$

where x and y represents coordinate axes along the continuous surface in the direction of motion and normal to it, respectively. u and v are the velocity components along the x and y axes, respectively. υ - kinematic viscosity, k_1 – thermal concuctivity, ρ_f - the density of the base fluid, σ - electrical conductivity, B_0 - magnetic field, ρ_p - the density of the nanoparticle, $(\rho c)_f$ - heat capacity of the fluid, D_B - the Brownian diffusion and D_T - thermophoretic diffusion coefficient, T – temperature inside the boundary layer, $(\rho c)_p$ - effective heat capacity of a nanoparticle, ρ - the density, T_∞ - is the temperature far away from the sheet, $\alpha = (\frac{k}{(\rho c)_f}, \tau = \left(\frac{(c\rho)_p}{(c\rho)_f}\right),\ \upsilon = (\frac{\mu}{\rho_f})$.

Similarity transformations used in this problem are:

$$\eta = \sqrt{\frac{a}{\upsilon}}y, \qquad \psi = \sqrt{a\upsilon}xf(\eta), \qquad h(\eta) = \frac{\phi - \phi_\infty}{\phi_w - \phi_\infty} \tag{8}$$

We introduce the dimensionless quantities for the thermal boundary conditions as:

(i) In prescribed surface temperature case, n is the wall temperature parameter T_w is the wall temperature and A is constant. When $n = 0$, the thermal conditions become isothermal. The non-dimensional temperature in this case is

$$\theta(\eta) = \frac{T - T_\infty}{T_w - T_\infty} \tag{9}$$

(ii) The prescribed heat flux is considered to vary with distance x from the origin. In this case the non dimensional temperature is

$$g(\eta) = \frac{T - T_\infty}{T_w - T_\infty} \tag{10}$$

Where $T_w - T_\infty = (\frac{Dx^s}{k})\sqrt{\frac{\upsilon}{a}}$, D is a constant.

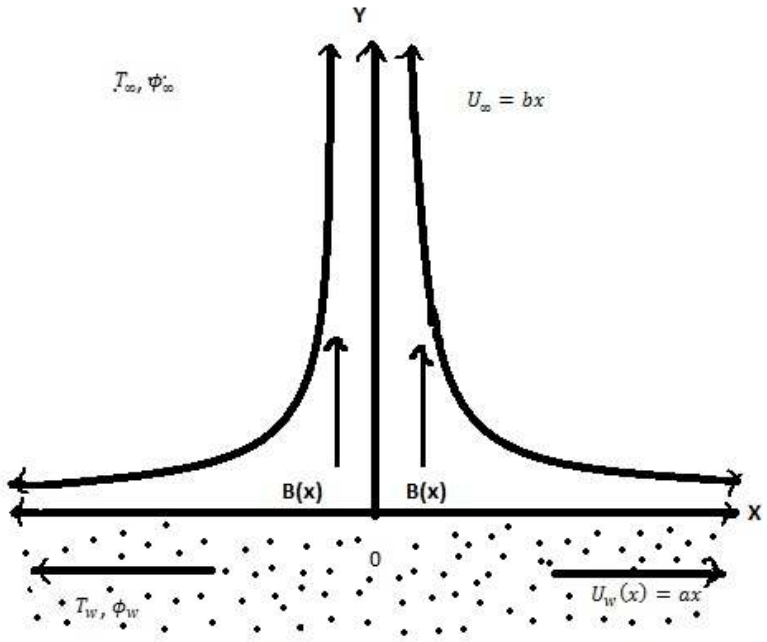

Fig. 1. Physical modal and coordinate system

The equation of continuity is satisfied if we choose a stream function $\psi(x,y)$ such that

$$u = \frac{\partial \psi}{\partial y}, \quad v = -\frac{\partial \psi}{\partial x} \tag{11}$$

By using the Rosseland approximation for radiation, we write the radiative heat flux as:

$$q_r = -\frac{4\sigma^*}{3k^*}\frac{\partial T^4}{\partial y} \tag{12}$$

where k^* is the mean absorption coefficient and σ^* is the Stefan-Boltzmann constant. Since the temperature differences within the flow field are assumed to be small, and then we linearize and expand T^4 into the Taylor series about T_∞, which after neglecting higher order forms takes the form

$$T^4 = 4T_\infty{}^3 T - 3T_\infty{}^4 \tag{13}$$

From above equation we get

$$q_r = -\frac{16T^3{}_\infty \sigma^*}{3k^*}\frac{\partial T}{\partial y} \tag{14}$$

Using the above transformations, the non-dimensional, nonlinear, and coupled ordinary differential equations are written as

(i) For PST case

$$f''' + ff'' - (f')^2 - (M+G)f' + M.S + S^2 = 0 \tag{15}$$

$$(1+R)\theta'' + Pr.f\theta' - n.Pr.f'\theta + Pr.Nb.hhhh'\theta' + Pr.Nt\theta'^2 = 0, \tag{16}$$

$$h'' + Le.fh' + \left(\frac{Nt}{Nb}\right).\theta'' = 0. \tag{17}$$

The transformed boundary conditions

$$f(0) = 0,\ f'(0) = 1,\ \theta(0) = 1,\ h(0) = 1,\ at\ \eta = 0,$$
$$f'(\infty) = S,\ \theta(\infty) = 0,\ h(\infty) = 0,\ as\ \ \eta \to \infty, \tag{18}$$

(ii) For PHF case

$$f''' + ff'' - (f')^2 - (M+G)f' + M.S + S^2 = 0 \tag{19}$$

$$(1+R)g'' + Pr.fg' - s.Pr.f'g + Pr.Nb.h'g' + Pr.Ntg'^2 = 0, \tag{20}$$

$$h'' + Le.fh' + \left(\frac{Nt}{Nb}\right).g'' = 0. \tag{21}$$

The transformed boundary conditions

$$f(0) = 0,\ f'(0) = 1,\ g'(0) = -1,\ h(0) = 1,\ at\ \eta = 0,$$
$$(\infty) = S,\ g(\infty) = 0,\ h(\infty) = 0,\ as\ \ \eta \to \infty, \tag{22}$$

Where $S = \frac{b}{a}$ is the velocity ratio, $Pr = \frac{\upsilon}{\alpha}$ is the Prandtl number, $R = \frac{16\sigma^* {T^3}_\infty}{3k^* k}$ is the radiation parameter, $M = \frac{\sigma {B_0}^2}{\rho_f a}$ is Magnetic parameter, $Nb = \frac{\tau D_B(\phi_w - \phi_\infty)}{\upsilon}$ is Brownian motion parameter, $Nt = \frac{\tau D_T(T_w - T_\infty)}{\upsilon T_\infty}$ is Thermophoresis parameter, $Le = (\frac{\upsilon}{D_B})$ is Lewis number, $G =$ porosity parameter.

Because the parameter Nt depends on x, true similarity solution is not achieved. However, if the parameter A is proportional x^{-n} and parameter D is also proportional to x^{-s} , Nt becomes independent of x and a true similarity is realized.

Heat transfer coefficient and mass transfer coefficients are important physical parameters. They defined as,

$$Nu_x = \frac{Lq_w}{k(T_w - T_\infty)} = -\frac{L\left(\frac{\partial T}{\partial y}\right)_{y=0}}{(T_w - T_\infty)}, \text{ and}$$

$$Sh_x = \frac{Lq_m}{k(\phi_w - \phi_\infty)} = -\frac{L\left(\frac{\partial \phi}{\partial y}\right)_{y=0}}{\phi_w - \phi_\infty}.$$

The dimensionless forms of these parameters are:

$$Nu_x = -(1+R)\sqrt{\frac{Re_x}{2}}\,\theta'(0), \text{ and } Sh_x = -\sqrt{\frac{Re_x}{2}}h'(0), \quad (23)$$

where the surface heat flux $q_w = k\left(\frac{\partial T}{\partial y} + \frac{\partial q_r}{\partial y}\right)_{y=0}$, the surface mass flux $q_m = k\left(\frac{\partial \phi}{\partial y}\right)_{y=0}$ and $Re_x = \frac{U_w L}{\upsilon}$ is the Reynolds number where k is the thermal conductivity. The numerical values of $-h'(0)$ are proportional to local Sherwood number and these are presented by Table 1 for the values of the physical parameters.

2.1 Numerical Solution

Equations (15)-(17) and (19)-(21) subjected to the boundary conditions (18) and (22) are solved numerically using finite difference method that is known as Keller box in combination with the Newton's techniques.

- Reducing higher order ODEs in to systems of first order ODEs
- Writing the systems of first order ODEs into difference equations using central differencing scheme
- Linearizing the difference equations using Newton's method and wring it in vector form
- Solving the system of equations using block elimination method

In order to solve the above differential equations numerically, we adopt function bvp4c in Matlab software which is very efficient in using the well known Keller box method. In accordance with the boundary layer analysis, the boundary condition at $\eta = \infty$ is replaced by $\eta = 4$, and the step size $\Delta\eta = 0.04$ is used to obtain numerical solution with four decimal place accuracy as the criterion of convergence. Obtained ordinary non-linear Equations are solved by Keller box method for boundary condition. Accuracy of this numerical method shown in Table 1 is being validated by direct comparison with the numerical results reported by Ibrahim and Shankar [22]. The numerical calculations of $\theta(0)$, and $-h'(0)$ for the values of Pr, Le, n, s, S, R, Nt, Nb, M, and G are shown in Table 2.

Table 1. Comparison of results for $-h'(0)$with previous published works

Pr	Wubshet Ibrahim [22]	Present work
1.0	0.9383	0.9383
2.0	0.8964	0.8964
5.0	0.8605	0.8605

Table 2. Showing results of $\theta(0)$ and $-h'(0)$ for the values of Pr, M, S, Le, R, s, Nt, Nb and G

Pr	S	Le	$\theta(0)$	$-h'(0)$
1	1	5	1.3650	1.3272
2	1	5	1.0097	1.2710
5	1	5	0.7099	1.2028
5	0	5	0.8598	0.7537
5	2	5	0.6096	1.5489
5	3	5	0.5398	1.8368
1	1	10	1.3810	2.1379
1	1	15	1.3889	2.7464
1	1	20	1.3939	3.2542

3. RESULTS AND DISCUSSION

In order to get a physical insight into the problem, a representative set of numerical results is shown graphically in Figs.2-15, to illustrate the influence of physical parameters viz., the magnetic parameter M, viscous ratio S, radiation parameter R, Prandtl number Pr, Brownian motion parameter Nb, thermophoresis parameter Nt, porosity parameter G, Lewis number Le on the velocity $f'(\eta)$, temperature $\theta(\eta)$ and concentration $h(\eta)$.

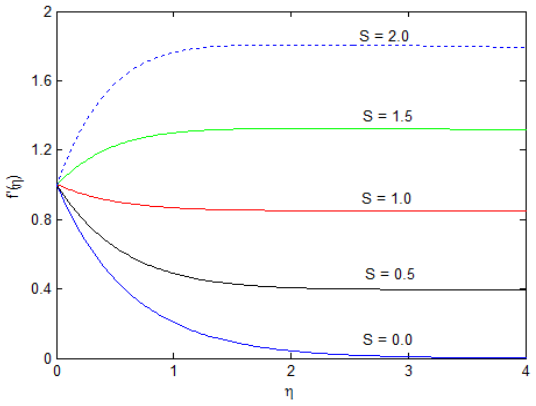

Fig. 2. Influence of S on $f'(\eta)$

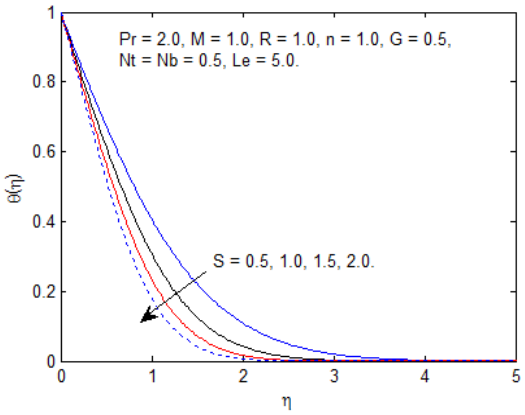

Fig. 3. Influence of S on $\theta(\eta)$

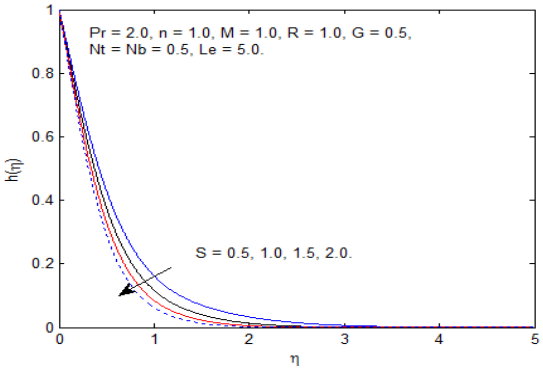

Fig. 4. Influence of S on $h(\eta)$

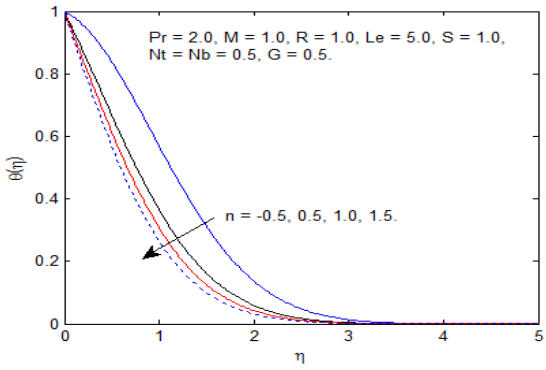

Fig. 5. Influence of n on $\theta(\eta)$

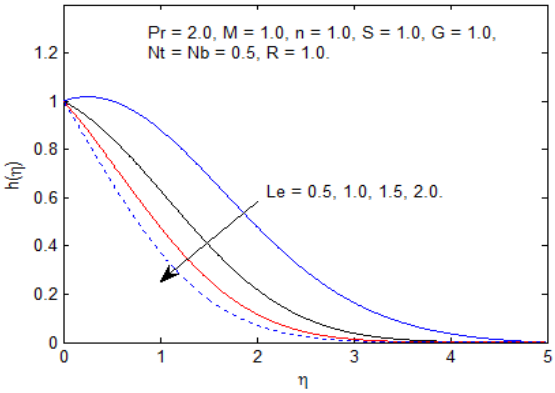

Fig. 6. Influence of Le on $h(\eta)$

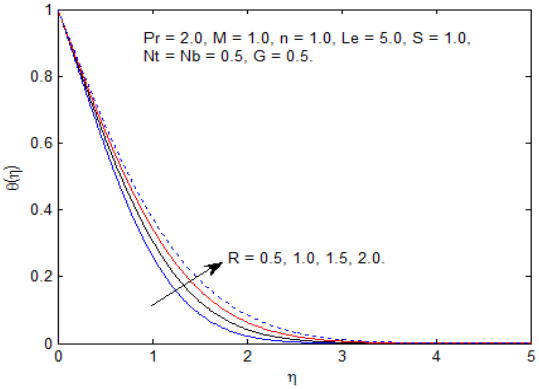

Fig. 7. Influence of R on $\theta(\eta)$

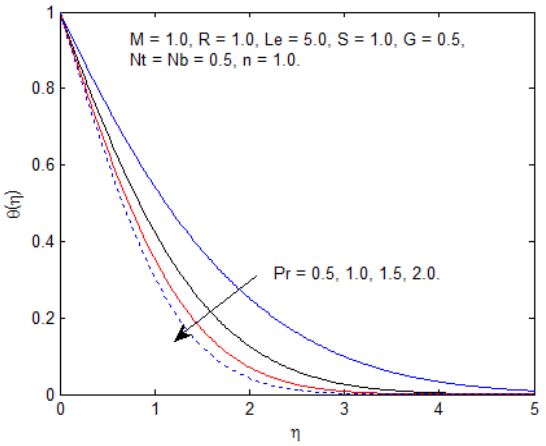

Fig. 8. Influence of Pr on $\theta(\eta)$

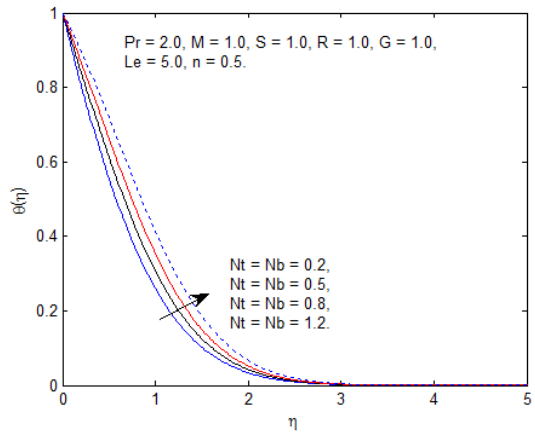

Fig. 9. Influence of Nb and Nt on $\theta(\eta)$

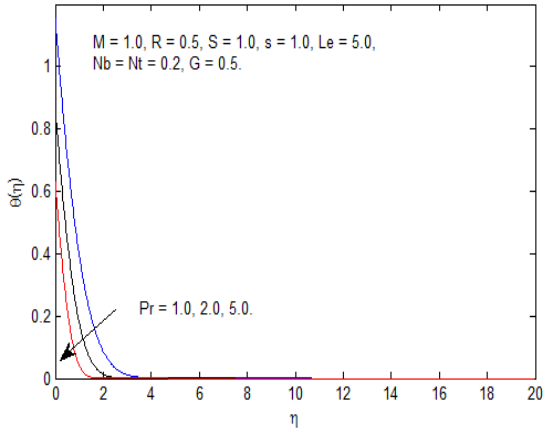

Fig. 10. Influence of Pr on $\theta(\eta)$

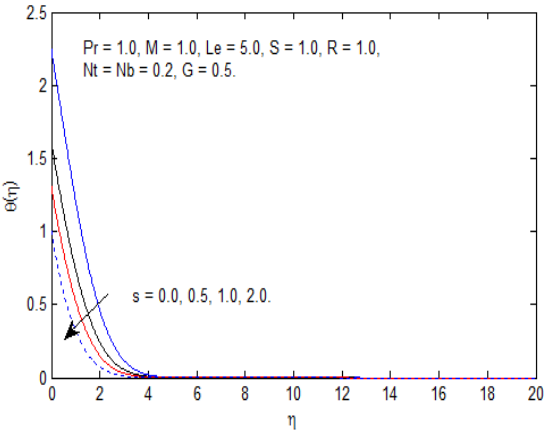

Fig. 11. Influence of s on $\theta(\eta)$

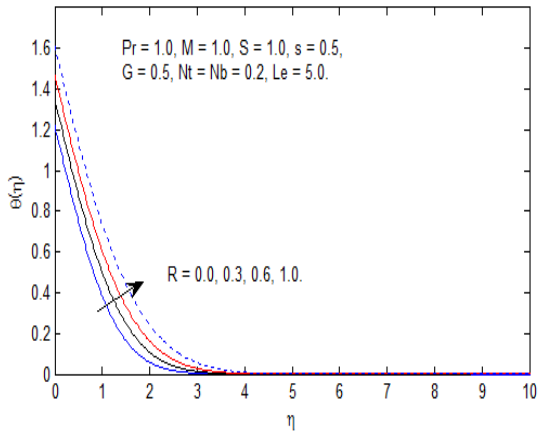

Fig. 12. Influence of R on $\theta(\eta)$

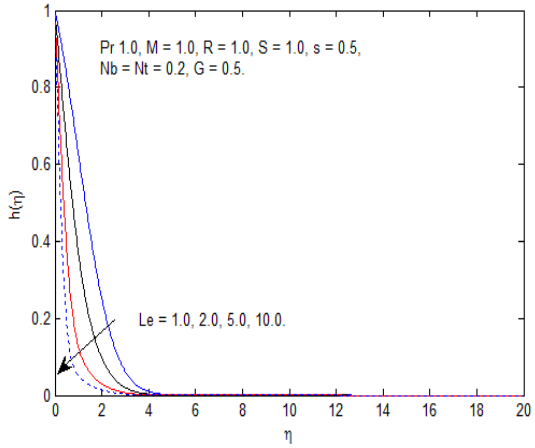

Fig. 13. Influence of Le on $h(\eta)$

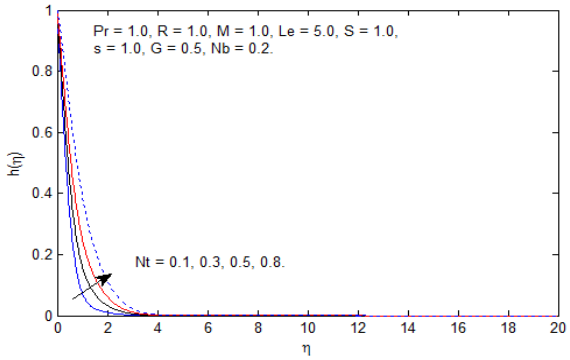

Fig. 14. Influence of Nt on $h(\eta)$

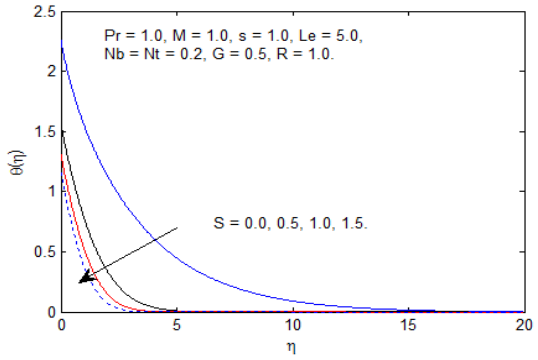

Fig. 15. Influence of S on $\theta(\eta)$

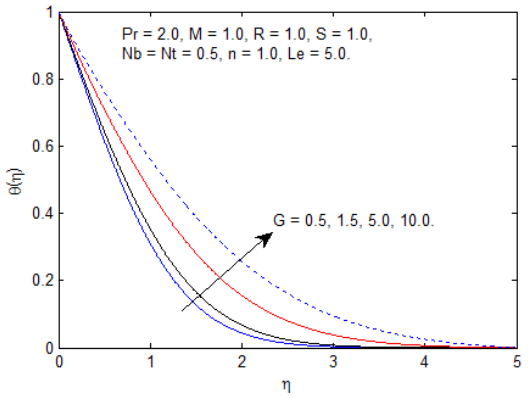

Fig. 16. Influence of G on $\theta(\eta)$

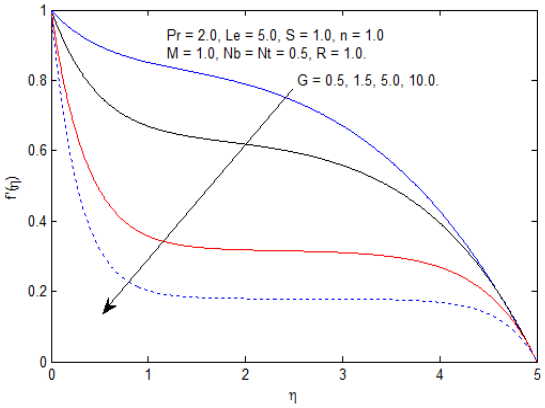

Fig. 17. Influence of G on $f'(\eta)$

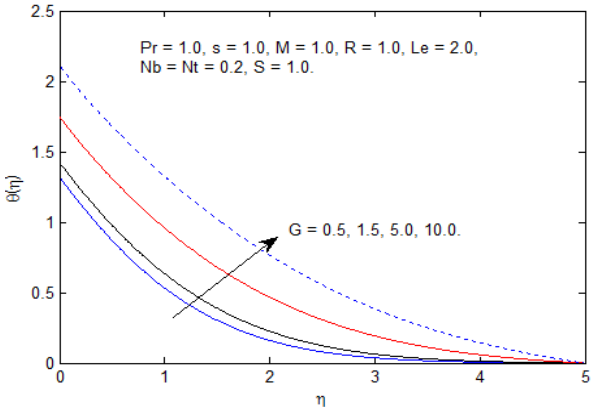

Fig. 18. Influence of G on $\theta(\eta)$

Fig. 2 refers that there is an increase in the velocity with an increase in velocity ratio S for some fixed values of parameters. It is evident from this figure that when $S < 1$, the thickness of the boundary layer decreases with the increase in S. Here is straining motion near the stagnation region increases so the acceleration of the external stream increases which causes a reduction in the boundary layer thickness and as a consequence the horizontal velocity increases. On the other hand, when $S > 1$, the flow has an inverted boundary layer structure. Here the sheet velocity $U_w(x) = ax$ exceeds the velocity of external stream $U_\infty(x) = bx$. It is also noticed that boundary layer is not formed when $S = 1$.

Fig. 3 depicts the effect of velocity ratio S on the temperature. The temperature and the thermal boundary layer thickness decrease with an increase in S.

Fig. 4 shows that the influence of S on the nanoparticles concentration is virtually similar to that accounted for the temperature $\theta(\eta)$.

Fig. 5 illustrates the effects of power index n of terms in non-isothermal surface. From the graph, we can realize that as the values of n increase, the temperature decreases and the thermal boundary layer thickness decreases.

Fig. 6 exhibits the nature of concentration field for the variation of Lewis number. As Lewis number increases the concentration graph decreases and the concentration boundary layer thickness decreases. This is probably due to the fact that mass transfer rate increases as Lewis number increases. It also reveals that the concentration gradient at surface of the sheet increases. Moreover, the concentration at the surface of a sheet decreases as the values of Le increase.

As depicted in Fig. 7, 12 it is noticed that an increase in R yields an increase in the nanofluid's temperature, which leads to decrease in the heat transfer rate. Thus, the radiation should be at its minimum in order to facilitate the cooling process. All these physical behaviour are due to the combined effects of the strength of the Brownian motion and thermophoresis particle deposition.

Figs. 8, 10, portrays the behaviour of Prandtl number Pr on the temperature. An increase in Pr rapidly shifts the profiles towards the boundary causing a diminution in the thickness of thermal boundary layer. A bigger Prandtl number has a relatively lower thermal diffusivity. Thus an increase in Pr reduces conduction and thereby increases the variation in the thermal characteristics. As expected, the variation in the temperature is more pronounced for smaller values of Pr than its larger values.

Fig. 9 is plotted to perceive the effects of Brownian motion and thermophoresis parameters on the temperature. There is a substantial increase in the temperature and the thermal boundary layer thickness with an increase in Nb and Nt. In nanofluid system, due to the presence of nanoparticles, the Brownian motion takes place and for the increase in Nb the Brownian motion is effected and consequently the heat transfer characteristics of the fluid changes. With increase of Nt, the temperature of the fluid increases. The over shoot near the wall is found. Increase in Nt causes increase in the thermophoresis force which tends to move nanoparticles from hot to cold areas and consequently it increases the magnitude of temperature profiles.

Fig. 11 illustrates the effects of power index s of terms in non-isothermal surface. From the graph, we can realize that as the values of s increase, the temperature decreases and the thermal boundary layer thickness decreases.

As it is noticed from Fig. 13 as Lewis number increases the concentration graph decreases and the concentration boundary layer thickness decreases. This is probably due to the fact that mass transfer rate increases as Lewis number increases. It also reveals that the concentration gradient at surface of the sheet increases. Moreover, the concentration at the surface of a sheet decreases as the values of Le increase.

Fig. 14 plots the concentration profiles for different values of the Thermophoresis parameter Nt. Here concentration boundary layer reduces as Nt increases which thereby enhances the nanoparticles concentration at the sheet.

Fig. 15 shows the effect of velocity ratio S on the temperature. The temperature and the thermal boundary layer thickness decrease with an increase in S.

Figs. 16, 17 and 18, shows the effect of porosity parameter G on the temperature and velocity profiles. It is observed that the presence of the porous medium. The temperature profile whereas is reduces the velocity profile. This is because the porous medium inhibits the fluid not to move freely through the boundary layer. This leads the flow to increase thermal boundary layer thickness.

4. CONCLUSIONS

In this work, the MHD stagnation point flow and heat transfer of nanofluid over a non-isothermal stretching sheet in porous medium is analyzed. The governing boundary layer equations are converted into highly nonlinear coupled similarity equations using linear group of transformation before being solved numerically. Numerical results were obtained using the function bvp4c in

MATLAB for several ranges of parameters: Magnetic parameter M, velocity ration S, temperature index parameter n, Prandtl number Pr, radiation parameter R, Lewis number Le, porosity parameter G, Brownian motion parameter Nb, thermophoresis parameter Nt. The main observations of the present study are as follows.

- An increase in velocity ratio S is to increase the velocity profile but is to decrease the temperature and concentration profiles
- As magnetic parameter M increases, velocity profile decreases
- An increase in radiation parameter R leads the temperature profiles to increase
- As n, increases, temperature and concentration profiles decreases
- The impact of Prandtl number shows that temperature profile is decreasing
- As Nt and Nb increases, the temperature of nanofluid increases, and as Nt increases, concentration decreases
- As s, increases, temperature profile decreases
- As increase in Nt is to increase the concentration profiles
- Lewis number Le reduces the concentration of nanofluid
- Porosity parameter G reduces the velocity of nanofluid, and increases the temperature of nanofluid.

COMPETING INTERESTS

Authors have declared that no competing interests exist.

REFERENCES

1. Choi SUS. Enhancing thermal conductivity of fluids with nanoparticles, proceedings of the ASME International Mechanical Engineering Congress. San Francisco, USA, ASME, FED 231/MD. 1995;66:99-105.
2. Masuda H, Ebata A, Teramae K, Hishinuma N, Alternation of thermal conductivity and viscosity of liquid by dispersing ultra-fine particles (dispersion of- $Al2O3$, $SiO2$ and $TiO2$ ultra-fine particles), Netsu Bussei (Japan). 1993;4: 227-233.
3. Buongiorno J, Convective transport in nanofluids. ASME J. Heat Transf. 2006; 128:240–250.
4. Eldabe Nabil TM, Mohamed Mona AA, Heat and mass transfer in hydromagnetic flow of the non-Newtonian fluid with heat source over an accelerating surface through a porous medium. Chaos, Solutions and Fractals. 2002;13:907-917.
5. Hamad MA, Ferdows M, Similarity solution of boundary layer stagnation-point flow towards a heated porous stretching sheet saturated with a nanofluid with heat absorption/generation and suction/blowing: A lie group analysis, Common on linear Sci Numer Simulat. 2011;17(1):132-140.
6. Fadzilah M, Nazar R, Norihan M, Pop I. MHD boundary layer flow and heat transfer over a stretching sheet with induced magnetic field. J. Heat Mass Transfer. 2011;47:155–162,.
7. Ishak A, Nazar R, Pop I. Hydro magnetic flow and heat transfer adjacent to a stretching vertical sheet. Heat Mass Transfer. 2008;44:921-927.
8. Mahapatra TR, Gupta AS, Magnetohydro-dynamics Stagnation Point Flow Towards a Stretching Sheet, Acta Mech. 2001;152: 191–196.
9. Ishak A, Jafar K, Nazar R, Pop I, MHD stagnation point flow towards a stretching sheet. Physica A. 2009;388:3377–3383.
10. Mabood F, Khan WA, Ismail AIM. MHD boundary layer flow and heat transfer of nanofluids over a nonlinear stretching sheet: A numerical study. Journal of Magnetism and Magnetic Materials. 2015; 374:569-576.
11. Khan ZH, Khan WA, Qasim M, Shah IA, MHD stagnation point ferrofluid flow and heat transfer toward a stretching sheet, IEEE Trans. Nanotechnol. 2014;13(1):35-40.
12. Shateyi S, Makinde OD, Hydromagnetic stagnation-point flow towards a radially stretching convectively heated disk, Math. Probl. Eng; 2013. Article ID 616947.
13. Aman F, Ishak A, Pop I, Magnetohydrodynamic stagnation-point flow towards a stretching/shrinking sheet with slip effects. Int. Commun. Heat Mass Transf. 2013;47:68-72.
14. Singh G, Makinde OD. MHD slip flow of viscous fluid over an isothermal reactive stretching sheet. Ann. Fac. Eng. Hunedoara Int. J. Eng. 2013;11(2):41-46.
15. Shateyi S, Marewo GT. Numerical analysis of unsteady MHD flow near a stagnation point of a two-dimensional porous body with heat and mass transfer, thermal

transfer, and chemical reaction. Bound. Value Probl. 2014;218.

16. Hayat T, Abbas Z, Pop I, Asghar S, Effects of radiation and magnetic field on the mixed convection stagnation-point flow over a vertical stretching sheet in a porous medium. International Journal of Heat and Mass Transfer. 2010;53:466-474.
17. Ibrahim W, Shankar B. MHD boundary layer flow and heat transfer of a nanofluid past a permeable stretching sheet with velocity, thermal and solutal slip boundary conditions. J. Comput. Fluids. 2013;75:1-10.
18. Nazar R, Amin N, Pop I. Unsteady mixed convection boundary layer flow near the stagnation point on a vertical surface in a porous medium. International Journal of Heat and Mass transfer. 2004;47:2681-2688.
19. Swathi M, Iswar Chandra M, Rama Subba Reddy G. MHD flow and heat transfer past a porous stretching non-isothermal surface in porous medium with variable free stream temperature. Thermal Energy and Power Engineering. 2013;2:29-37.
20. Datti PS, Prasad KV, Subhas Abel M, Ambuja Joshi. MHD visco-elastic fluid flow over a non-isothermal stretching sheet. International Journal of Engineering Science. 2004;42:935-946.
21. Prasad KV, Subhas Abel M, Sujith Kumar Khan. Momentum and heat transfer in visco-elastic fluid flow in a porous medium over a non-isothermal stretching sheet. International Journal of Numerical Methods for Heat & Fluid Flow. 2000;10:786–801.
22. Wubshet Ibrahim, Shankar B. Magneto hydrodynamic Boundary Layer Flow and Heat Transfer of a Nanofluid over Non-Isothermal Stretching Sheet, Journal of Heat Transfer. 2014;136: 051701/1-9.

Peer-review history:
The peer review history for this paper can be accessed here:
http://sciencedomain.org/review-history/16924